



Ultrahigh accelerating gradient and quality factor of CEPC 650 MHz superconducting radio-frequency cavity

Peng Sha^{1,2,3,4} · Wei-Min Pan^{1,2,3,4} · Song Jin^{1,2,3} · Ji-Yuan Zhai^{1,2,3,4} · Zheng-Hui Mi^{1,2,3,4} · Bai-Qi Liu^{1,2,3} · Chao Dong^{1,2,3} · Fei-Si He^{1,2,3,4} · Rui Ge^{1,2,3,4} · Liang-Rui Sun^{1,2,3} · Shi-Ao Zheng^{1,2,3,4} · Ling-Xi Ye^{1,2,3,4}

Received: 24 July 2022 / Revised: 1 September 2022 / Accepted: 11 September 2022 / Published online: 10 October 2022
© The Author(s), under exclusive licence to China Science Publishing & Media Ltd. (Science Press), Shanghai Institute of Applied Physics, the Chinese Academy of Sciences, Chinese Nuclear Society 2022

Abstract Two 650 MHz single-cell superconducting radio-frequency (SRF) cavities used for the Circular Electron Positron Collider (CEPC) were studied to achieve a high accelerating gradient (E_{acc}) and high intrinsic quality factor (Q_0). The 650 MHz single-cell cavities were subjected to a combination of buffered chemical polishing (BCP) and electropolishing (EP), and their E_{acc} exceeded 40 MV/m. Such a high E_{acc} may result from the cold EP with more uniform removal. BCP is easy, cheap, and rough, whereas EP is complicated, expensive, and precise. Therefore, the combination of BCP and EP investigated in this study is suitable for surface treatments of mass SRF cavities. Medium temperature (mid-T) furnace baking was also conducted, which demonstrated an ultrahigh Q_0 of 8×10^{10} at 22 MV/m for both cavities, and an extremely

low BCS resistance (R_{BCS}) of $\sim 1.0 \text{ n}\Omega$ was achieved at 2.0 K.

Keywords SRF cavity · Accelerating gradient · Quality factor · Electropolishing · Vertical test

1 Introduction

Superconducting radio-frequency (SRF) cavities are widely used in modern particle accelerators [1], including high-energy colliders [2, 3], synchrotron light sources [4], free electron lasers [5–7], and proton/neutron sources [8–12]. SRF cavities made of niobium, which has a high residual resistance ratio (RRR), and exhibiting a high accelerating gradient (E_{acc}) and high intrinsic quality factor (Q_0) are required for such accelerators. Therefore, many technologies and approaches have been studied to improve the E_{acc} and Q_0 of SRF cavities; these approaches include the International Linear Collider (ILC) recipe, nitrogen doping, and mid-T baking [13–17]. The electropolishing (EP) technique has been developed into a standard treatment for the 1.3 GHz 9-cell cavity for the ILC and is known as “the ILC recipe”. The maximum E_{acc} of 1.3 GHz 9-cell cavities achieved using the ILC recipe exceeds 40 MV/m, which is remarkably high for SRF cavities [5, 18, 19]. The 2/0 recipe (two minutes of nitrogen exposure followed by zero minutes of annealing at 800 °C in a furnace) was used for the nitrogen doping of 1.3 GHz 9-cell cavities for the Linac Coherent Light Source II High Energy. Consequently, the Q_0 of the cavities was improved to 3.0×10^{10} at 21 MV/m, which is higher than the specification of the Linac Coherent Light Source II (2.7×10^{10} at 16 MV/m) [20]. Moreover, following mid-T

This work was supported by the Strategic Priority Research Program of the Chinese Academy of Sciences (No. XDB25000000), the National Natural Science Foundation of China (No. 12075270), and the Platform of Advanced Photon Source Technology R&D.

✉ Peng Sha
shapeng@ihep.ac.cn

✉ Wei-Min Pan
panwm@ihep.ac.cn

¹ Institute of High Energy Physics, Chinese Academy of Sciences, Beijing 100049, China

² Key Laboratory of Particle Acceleration Physics and Technology, Chinese Academy of Sciences, Beijing 100049, China

³ Center for Superconducting RF and Cryogenics, Institute of High Energy Physics, Chinese Academy of Sciences, Beijing 100049, China

⁴ University of Chinese Academy of Sciences, Beijing 100049, China

furnace baking, the Q_0 of 1.3 GHz 9-cell cavities reached 3.8×10^{10} at 16 MV/m on average at the Institute of High Energy Physics (IHEP), Chinese Academy of Sciences [21]. Thus, exceptionally high E_{acc} and Q_0 have been achieved for the 1.3 GHz 9-cell cavities.

The Circular Electron Positron Collider (CEPC), which was proposed by the IHEP in 2012, is a 100-km collider with a center-of-mass energy of 90–240 GeV for Z, W, and Higgs bosons [22]. Precise measurements of the Higgs boson are considered critical for developments in high-energy physics. The CEPC is capable of producing 1,000,000 Higgs bosons within 10 years and is regarded as a Higgs factory. The SRF system of the CEPC is critical and challenging owing to the wide range of beam energies and currents [23]. The booster ring of CEPC adopts 1.3 GHz 9-cell cavities, as well as E-XFEL and ILC. The collider ring of the CEPC adopts hundreds of 650 MHz SRF cavities operated in the continuous wave (CW) mode [24], which compensate for the loss of beam energy resulting from synchrotron radiation. Large elliptical (< 1 GHz) cavities with high E_{acc} and Q_0 have been widely adopted for accelerator applications, such as in the European Spallation Source (ESS) [8], Facility Rare Isotope Beams (FRIB) [9], Spallation Neutron Source (SNS) [10], Proton Improvement Plan II (PIP-II) [12], Beijing Electron Positron Collider II (BEPC II) [25], and the China initiative Accelerator Driven System (CiADS) [26]. However, they have not been studied as extensively as 1.3 GHz cavities. The operation specification of 805 MHz cavities with $\beta = 0.81$ for SNS is 5.0×10^9 @ 15.8 MV/m at 2.1 K [10], whereas the operation specification of 704.42 MHz cavities with $\beta = 0.86$ for ESS is 5.0×10^9 @ 19.9 MV/m at 2.0 K [27]. The 650 MHz cavities with $\beta = 0.92$ for PIP-II require a Q_0 of 3.0×10^{10} at 18.8 MV/m (at 2.0 K), which indicates a requirement of a higher Q_0 than that required for ESS and SNS [12]. Finally, the 650 MHz cavities with $\beta = 1$ for CEPC require a Q_0 of 4×10^{10} at 22 MV/m during the vertical test (VT) at 2.0 K; these specifications are difficult to realize compared with those of other cavities.

In the past, large elliptical cavities were mostly processed using buffered chemical polishing (BCP), which met the specifications for projects such as ESS and SNS. BCP is more convenient and simpler than EP. However, the surface roughness of SRF cavities processed by BCP is almost an order of magnitude higher than that processed by EP; thus, achieving high E_{acc} by BCP is difficult [28–30]. Hence, cavities processed by BCP could not consistently exceed the specifications of the 650 MHz cavities for PIP-II and CEPC, whereas those processed by EP could achieve higher E_{acc} and Q_0 . After the EP process, the 650 MHz single-cell cavity of PIP-II reached a maximum E_{acc} of ~ 37 MV/m at the Fermi National Accelerator

Laboratory (FNAL), which is an ultrahigh value for large elliptical cavities [12]. However, EP is complicated to perform and is expensive. Thus, the combination of BCP and EP may be efficient and convenient for large elliptical cavities with high E_{acc} and Q_0 . Therefore, validating the “BCP + EP” recipe for 650 MHz cavities is of considerable interest for our research. In our study, two 650 MHz single-cell cavities for CEPC were processed by BCP and EP, both of which exceeded the E_{acc} of 40 MV/m.

The remainder of this paper is organized as follows. Section 2 briefly describes the materials used, fabrication, BCP process, and vertical test results of 650 MHz single-cell cavities. Section 3 describes the 1st EP process and discusses the performance of the 650 MHz single-cell cavities. Section 4 describes the mid-T furnace baking implemented after the 1st EP process. The 2nd EP process (cold EP) and the performance of the cavities are discussed in detail in Sect. 5. Finally, the conclusions of this study are presented in Sect. 6.

2 BCP process

The two 650 MHz single-cell cavities, 650S4 and 650S5, investigated in this study, were made of fine-grain niobium, except for the flanges made of niobium–titanium (NbTi) alloy. The main parameters of the fine-grain niobium are listed in Table 1. The cavity components were formed by deep drawing and joined by electron beam welding. After fabrication, 650S4 and 650S5 were subjected to the same surface treatments, i.e., bulk BCP (~ 200 μm), high-temperature annealing at 800 °C for 3 h, and light BCP (~ 30 μm), all of which were conducted at Ningxia Orient Superconductor Technology Co., Ltd. (OSTEC). A mixture of hydrofluoric acid (HF), nitric acid (HNO_3), and orthophosphoric acid (H_3PO_4) in a ratio of 1:1:2 was adopted for the BCP process. Then, the cavities were transferred to the IHEP, where a high-pressure

Table 1 Main parameters of fine-grain niobium

Parameters	Values
RRR	350–400
ASTM size	5.0–5.5
HV10	~ 47.8
Yield strength (MPa)	63.9–67.4
Tensile ultimate strength (MPa)	167.5–173.1
Content of C (ppm)	7
Content of O (ppm)	7
Content of N (ppm)	8
Content of H (ppm)	1

water rinse (HPR), an assembly with flanges in a clean-room, and low-temperature baking (120 °C for 48 h) were performed. Uniform low-temperature baking was performed using a heating jacket, as shown in Fig. 1. Subsequently, vertical tests were conducted, as shown in Fig. 2. The residual magnetic field around the cavity was less than 5 mGs because of magnetic shielding inside the dewar [31, 32]. During the vertical tests, 650S4 and 650S5 were both quenched below an accelerating gradient of 25 MV/m, as shown in Fig. 3, along with a strong field emission. The accelerating voltage ($V_C = E_{\text{acc}} \times 0.23$) and surface peak RF magnetic field (B_{peak}) as well as E_{acc} are adopted as scales of the RF field in Fig. 3. For 650S4 and 650S5, the relation between B_{peak} and E_{acc} is expressed as follows: $B_{\text{peak}}/E_{\text{acc}} \approx 4.2$ mT/(MV/m). Thus, the Q_0 values of 650S4 and 650S5 were both lower than the CEPC VT specification of 4×10^{10} at 22 MV/m. Subsequently, 650S4 and 650S5 were subjected to the EP process.

3 1st EP process

The EP was performed at the OSTEC, too. The setup of the EP process for the 650 MHz single-cell cavity is depicted in Fig. 4. The electrolyte for the EP process was a mixture of HF and H₂SO₄ at a ratio of 1:9. Various acid flow rates were investigated in this study. Finally, a flow rate of 15 L/min was used. A nominal voltage of 21 V was adopted for the EP process. First, 650S5 was subjected to EP, and its inner surface was removed by ~ 215 μm at < 25 °C and ~ 100 μm at ~ 17.5 °C. Next, the surface of 650S4 was removed by ~ 20 μm by light EP at ~ 25 °C, followed by high-temperature annealing at 950 °C for 3 h; subsequently, another removal of ~ 20 μm by light EP at ~ 17.5 °C was performed again. The details are introduced in [24]. Subsequently, 650S4 and 650S5 were shipped to the IHEP, where the HPR, assembly

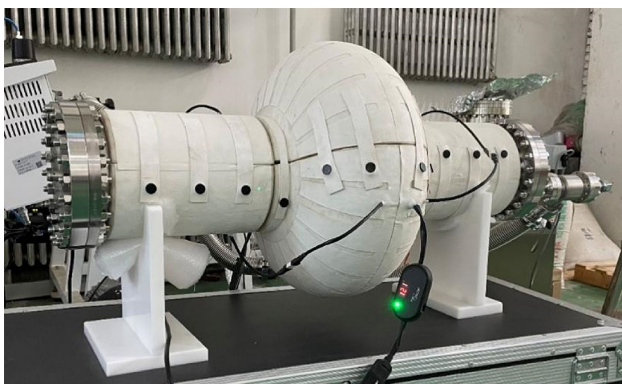


Fig. 1 (Color online) Low-temperature baking of 650 MHz single-cell cavity



Fig. 2 (Color online) Site photograph of vertical test of 650 MHz single-cell cavity

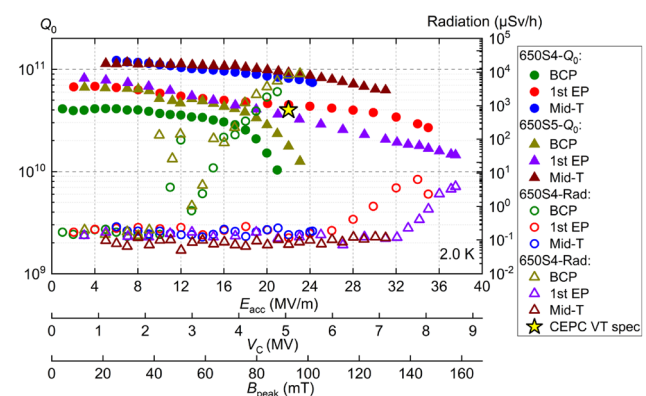


Fig. 3 (Color online) Vertical test results of 650S4 and 650S5, which demonstrate Q_0 and radiation versus accelerating gradient

with flanges, low-temperature baking (120 °C for 48 h), and vertical tests were conducted. Higher E_{acc} and Q_0 values were observed after the EP process, as shown in Fig. 3. 650S4 quenched at ~ 35.0 MV/m with a Q_0 of 2.7×10^{10} , whereas 650S5 quenched at ~ 37.5 MV/m with a Q_0 of 1.4×10^{10} . The combination of BCP and EP was effective for achieving a high E_{acc} and Q_0 [13]. Hence, bulk EP in the ILC recipe may be replaced by bulk BCP, which is favorable mass production and surface treatments



Fig. 4 (Color online) Setup of EP process of 650 MHz single-cell cavity

of SRF cavities. In addition, the Q_0 of 650S5 was slightly lower than that of 650S4 at a high gradient (> 20 MV/m), which may be because it was not subjected to high-temperature annealing [24]. Annealing can degas hydrogen trapped in niobium, thereby reducing the RF loss and increasing Q_0 of the SRF cavity [33].

Subsequently, 650S5 was again subjected to high-temperature annealing at 900°C for 3 h, which was aimed at hydrogen degassing. Next, the 650 MHz single-cell cavities were transferred to an ISO 6 cleanroom. The inner and outer surfaces of the cavities were manually rinsed with Liquinox solution (2%), followed by HPR, and then dried in the cleanroom.

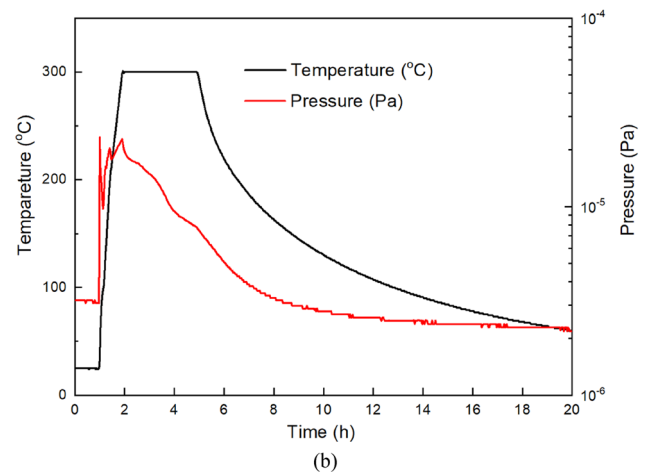
4 Mid-T furnace baking

Following drying, the 650 MHz single-cell cavities were transferred to a furnace for mid-T baking. The recipe of baking at 300°C for 3 h and 1.3 GHz cavities used in reference [21] were used. During the entire process, the cavities were supported by two niobium holders. The flanges of the cavities were covered with niobium foils, as shown in Fig. 5a, and were freshly polished chemically to prevent particles from entering the interior space of the cavities during the baking process. The vacuum and temperature curves during the mid-T furnace baking of 650S4 are shown in Fig. 5b. Prior to heating, the furnace was evacuated to an ultrahigh vacuum ($< 5 \times 10^{-6}$ Pa) using two cryopumps. The peak pressure reached $\sim 2.3 \times 10^{-5}$ Pa during the baking process. When the temperature dropped to $\sim 50^\circ\text{C}$, the pressure decreased to $\sim 2.1 \times 10^{-6}$ Pa, and the cavity was removed from the furnace. The mid-T furnace baking of 650S5 was identical to that of 650S4.

Following mid-T furnace baking, 650S4 and 650S5 were subjected to HPR, clean assembly with flanges, and vertical tests; low-temperature baking was not performed.



(a)



(b)

Fig. 5 (Color online) Mid-T furnace baking of 650 MHz single-cell cavity. **a** Setup of mid-T furnace baking for 650 MHz single-cell cavity with flanges covered by niobium foils; **b** vacuum and temperature curves during mid-T furnace baking of 650S4

The curves of Q_0 versus E_{acc} during the vertical tests are shown in Fig. 3. Both cavities demonstrated significantly high Q_0 values for all the RF fields. The Q_0 values of 650S4 and 650S5 exceeded 8.0×10^{10} at 22 MV/m, which was twice that of the CEPC VT specification (4.0×10^{10}). 650S5 achieved a high Q_0 of 6.4×10^{10} at 30 MV/m, which was a relatively high E_{acc} at this frequency. No field emissions were observed during the vertical tests of the 650S4 and 650S5. In addition, neither of the 650 MHz single-cell cavities demonstrated the anti- Q -slope behavior, which is typically observed in 1.3 GHz cavities subjected to mid-T baking [16, 17, 21]. Finally, 650S4 and 650S5 quenched at ~ 24.2 MV/m and ~ 31.2 MV/m, respectively. Thus, the maximum E_{acc} of the 650 MHz single-cell cavities subjected to mid-T furnace baking decreased substantially. In other words, mid-T furnace baking could increase the Q_0 of 650 MHz cavities but lowered the E_{acc} .

For the RF cavity, Q_0 is defined as $Q_0 = G/R_S$, where G denotes the geometric factor, and R_S denotes the surface resistance. For 650S4 and 650S5, G is 284Ω . Hence, the

Q_0 of 650 MHz single-cell cavities was enhanced after mid-T furnace baking, indicating a reduction in R_S . R_S consists of two parts: temperature-dependent resistance (R_{BCS}) and temperature-independent resistance (R_{res}) [33–35].

$$R_S = A \frac{f^2}{T} \exp\left(-\frac{\Delta T}{kT}\right) + R_{res} \quad (1)$$

The first term in the equation is R_{BCS} , which depends on the Boltzmann constant (k), temperature (T), resonant frequency of the SRF cavity (f), energy gap of the superconductor (2Δ), and the fitting constant (A). A depends on material parameters.

For the investigations of R_{BCS} and R_{res} , 650S4 was subjected to vertical tests at different temperatures below 2.0 K. The R_{BCS} at 2.0 K and R_{res} of 650S4 was calculated using Eq. (1), as shown in Fig. 6. The values were compared with those of the 1.3 GHz nine-cell cavity (N8), which was subjected to the EP process and mid-T furnace baking at 300 °C for 3 h [21]. The R_{BCS} of 650S4 was ~ 1 n Ω and remained constant as a function of E_{acc} and B_{peak} , similar to that of 650 MHz single-cell cavities subjected to nitrogen doping at FNAL [12]. The decrease in R_{BCS} as a function of the RF field for N8 was not reproduced for 650S4. It was observed that mid-T furnace baking and nitrogen doping could not reverse the R_{BCS} at the frequency of 650 MHz [12]. Therefore, the anti- Q -slope behavior could not be achieved for the 650 MHz cavity subjected to mid-T furnace baking. Therefore, the RF field dependence of R_{BCS} was correlated with the resonant frequency of the SRF cavity, which has been explained in detail in [34–36]. Furthermore, R_{res} increased gradually to ~ 2 n Ω with the RF field.

5 2nd EP process (cold EP)

Subsequently, 650S4 and 650S5 were subjected to 30 μm EP, aiming to eliminate mid-T furnace baking and reset the inner surface. The temperature for this 2nd EP was lower than that of the 1st EP and was maintained below ~ 13 °C; thus, it was called “cold EP”. Recently, it was found that cold EP could achieve uniform removal of a 1.3 GHz cavity, thereby improving the quench field [37, 38].

For 650 MHz single-cell cavities, the surface removal at the beam tubes, irises, and equators, represented by Nos. 1 – 6 in Fig. 7a, was measured during the EP process. Figure 7b presents the results of the 1st EP for 650S4, which indicate that the removal at the equators (3, 4) was less than that at the beam tubes (1, 6). Figure 7c shows the results of the 2nd EP for 650S4, which demonstrate that the removal at the equators (3, 4) was almost the same as that at the beam tubes (1, 6). Therefore, the cold EP could successfully achieve uniform removal of the 650 MHz cavities as well as the 1.3 GHz cavity.

After the 2nd EP process, the inner surfaces of 650S4 and 650S5 were examined. There were no apparent defects in either of the cavities. The surface of 650S4 was similar before and after the 2nd EP, as shown in Fig. 8. Both of the 650 MHz single-cell cavities were subsequently subjected to HPR, clean assembly with flanges, and low-temperature baking at 120 °C for 48 h, followed by vertical tests.

The vertical test results for samples 650S4 and 650S5 are shown in Fig. 9. The Q_0 values of both cavities decreased slightly as a function of E_{acc} , which is typical for cavities processed with EP. The high-field Q -slope (HFQS) phenomenon was not evident for either of the cavities.

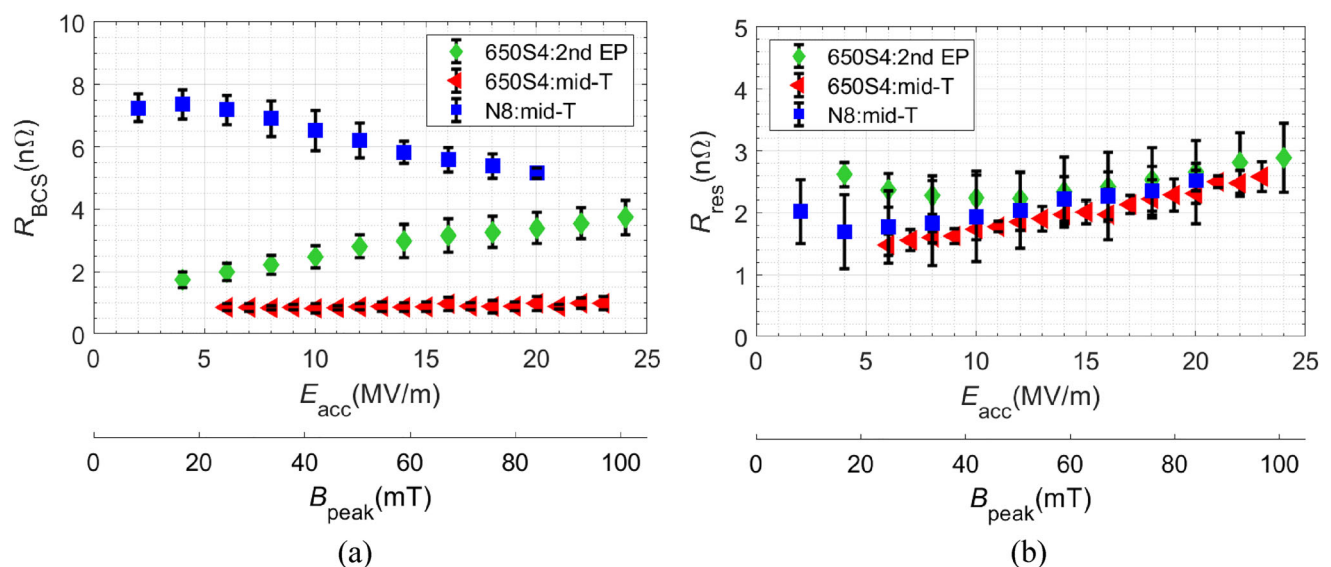


Fig. 6 (Color online) BCS resistance and residual resistance for 650S4 and N8. **a** R_{BCS} ; **b** R_{res}

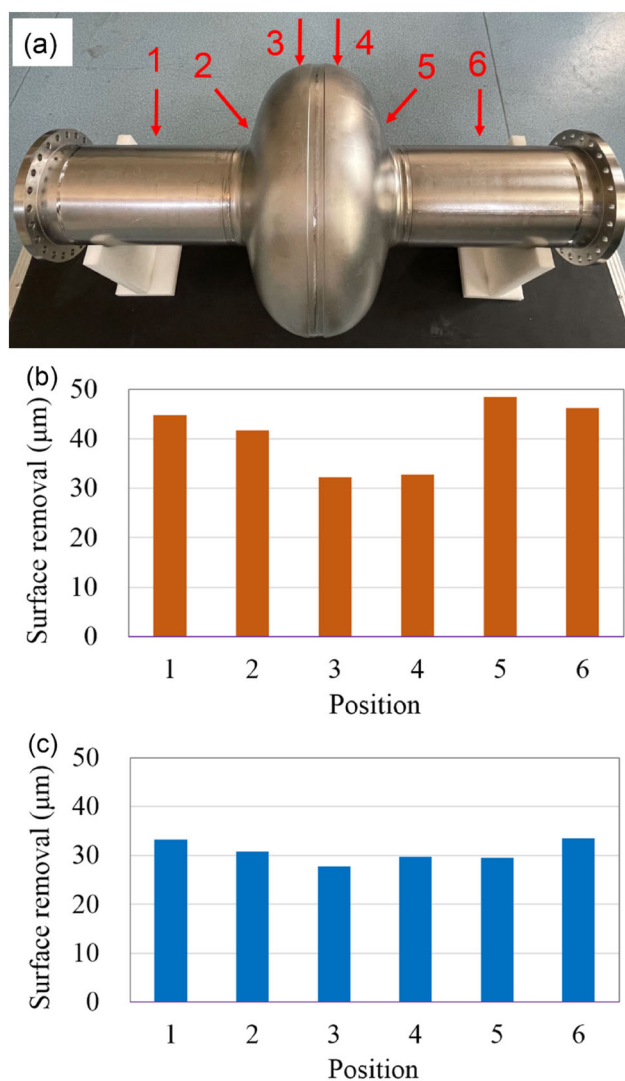


Fig. 7 (Color online) EP removal of 650S4: **a** red arrows and numbers indicate the locations where thickness was measured; **b** surface removal of the 1st EP; **c** surface removal of the 2nd EP

Finally, 650S4 and 650S5 achieved a higher gradient after the 2nd EP than after the 1st EP, and they quenched at ~ 41.0 MV/m ($B_{\text{peak}} \approx 172$ mT) with Q_0 of 1.5×10^{10} and ~ 41.6 MV/m ($B_{\text{peak}} \approx 175$ mT) with Q_0 of 2.3×10^{10} , respectively. The B_{peak} values of 650S4 and 650S5 were exceptionally high and exceeded the lower critical field ($B_{\text{C1}} = 170$ mT) of niobium. No field emission was observed during the vertical test of 650S4, which is rare for such large cavities. During the vertical test of 650S5, the field emission began to increase above a gradient of 37 MV/m and was weakly accompanied by X-ray radiation. In summary, a significantly high RF field was achieved by 650S4 and 650S5 during the vertical tests,

which indicated that the inner surfaces of both cavities were smooth and defect-free. Thus, the 2nd EP, HPR, assembly, low-temperature baking, and vertical tests for 650S4 and 650S5 were successful. This indicated that cold EP could enhance the quench RF field of 650 MHz cavities. Moreover, the values of Q_0 for 650S4 after the 1st and 2nd EP were almost the same.

The R_{BCS} and R_{res} values of 650S4 during the 2nd EP were also estimated, as shown in Fig. 6. R_{BCS} increased from ~ 2 n Ω at 4 MV/m to ~ 4 n Ω at 24 MV/m, which is higher than that achieved by mid-T furnace baking. Hence, 30 μm removal by the 2nd EP was sufficient to eliminate the effects of mid-T furnace baking. Moreover, R_{res} was between 2 and 3 n Ω , similar to the value after mid-T furnace baking.

6 Conclusion

State-of-the-art surface treatments for improving the performance of CEPC 650 MHz single-cell cavities were investigated in this study. The combination of BCP and EP was successfully applied to 650S4 and 650S5, both of which exceeded the accelerating gradient of 40 MV/m, which is remarkably high. Finally, 650S4 quenched at ~ 41.0 MV/m ($B_{\text{peak}} \approx 172$ mT) with $Q_0 = 1.5 \times 10^{10}$, whereas 650S5 quenched at ~ 41.6 MV/m ($B_{\text{peak}} \approx 175$ mT) with $Q_0 = 2.3 \times 10^{10}$. Previously, large elliptical cavities seldom exceeded the E_{acc} of 40 MV/m or B_{peak} of 170 mT, which is the lower critical magnetic field of niobium. BCP is easy but has low precision, whereas EP is complicated but has high precision. Therefore, the “BCP + EP” recipe is attractive and efficient for surface treatments of mass SRF cavities, such as CEPC, CiADS, and PIP-II.

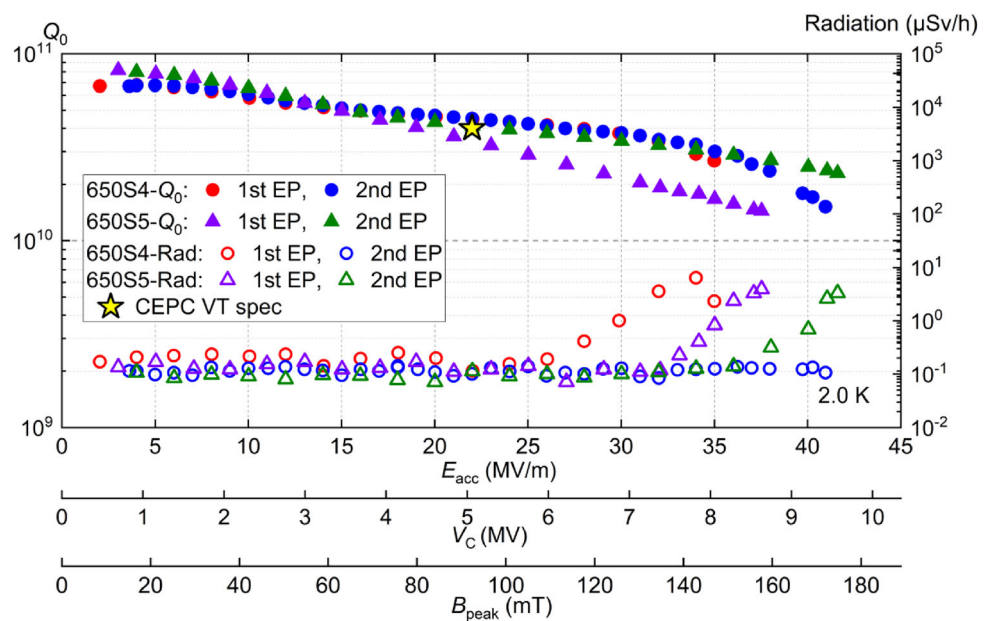
Mid-T furnace baking of 650S4 and 650S5 demonstrated ultrahigh quality factors at medium RF fields. Q_0 exceeded 8×10^{10} at 22 MV/m for both 650 MHz single-cell cavities. An extremely low R_{BCS} (~ 1.0 n Ω) was achieved at 2.0 K; this is a notable result. Moreover, the anti- Q -slope behavior was not observed, which is similar to that of nitrogen-doped 650 MHz cavities.

The research presented in this paper is beneficial for improving the performance and enhancing the fundamental understanding of P-band (0.23–1 GHz) elliptical cavities, which are of interest for next-generation high-energy colliders, proton sources, and synchrotron light sources. The surface treatments of the SRF cavity developed in this study are simplified and easy to replicate, which will benefit researchers working in the field of SRF.



Fig. 8 (Color online) Inner surface of 650S4 (cell). **a** Before the 2nd EP; **b** after the 2nd EP

Fig. 9 (Color online) Comparison of vertical test results of 650 MHz single-cell cavities



Author contributions All authors contributed to the study conception and design. Material preparation, data collection, and analysis were performed by Peng Sha, Wei-Min Pan, and Song Jin. The first draft of the manuscript was written by Peng Sha, and all authors commented on previous versions of the manuscript. All authors read and approved the final manuscript.

References

1. H. Padamsee, 50 years of success for SRF accelerators—a review. *Supercond. Sci. Technol.* **30**, 053003 (2017). <https://doi.org/10.1088/1361-6668/aa6376>
2. P. Sha, J.K. Hao, W.M. Pan et al., Nitrogen doping/infusion of 650 MHz cavities for CEPC. *Nucl. Sci. Tech.* **32**, 45 (2021). <https://doi.org/10.1007/s41365-021-00881-3>
3. T. Dohmae, K. Umemori, M. Yamanaka et al., Investigation of in-house superconducting radio-frequency 9-cell cavity made of large grain niobium at KEK. *Nucl. Instrum. Methods Phys. Res. A* **875**, 1–9 (2017). <https://doi.org/10.1016/j.nima.2017.08.050>
4. X.Y. Pu, H.T. Hou, Y. Wang et al., Frequency sensitivity of the passive third harmonic superconducting cavity for SSRF. *Nucl. Sci. Tech.* **31**, 31 (2020). <https://doi.org/10.1007/s41365-020-0732-x>
5. D. Reschke, V. Gubarev, J. Schaffran et al., Performance in the vertical test of the 832 nine-cell 1.3 GHz cavities for the European X-ray Free Electron Laser. *Phys. Rev. Accel. Beams* **20**, 042004 (2017). <https://doi.org/10.1103/PhysRevAccelBeams.20.042004>
6. Y.X. Zhang, J.F. Chen, D. Wang, RF design optimization for the SHINE 3.9 GHz cavity. *Nucl. Sci. Tech.* **31**, 73 (2020). <https://doi.org/10.1007/s41365-020-00772-z>

7. D. Gonnella, S. Aderhold, A. Burrill et al., Industrialization of the nitrogen-doping preparation for SRF cavities for LCLS-II. *Nucl. Instrum. Methods Phys. Res. A* **883**, 143–150 (2018). <https://doi.org/10.1016/j.nima.2017.11.047>
8. R. Garoby, A. Vergara, H. Danared et al., The European spallation source design. *Phys. Scr.* **93**, 014001 (2018). <https://doi.org/10.1088/1402-4896/aa9bff>
9. K. McGee, S. Kim, K. Elliott et al., Medium-velocity superconducting cavity for high accelerating gradient continuous-wave hadron linear accelerators. *Phys. Rev. Accel. Beams* **24**, 112003 (2016). <https://doi.org/10.1103/PhysRevAccelBeams.24.112003>
10. S.-H. Kim, R. Afanador, D. Barnhart et al., Overview of ten-year operation of the superconducting linear accelerator at the spallation neutron source. *Nucl. Instrum. Methods Phys. Res. A* **852**, 20–32 (2017). <https://doi.org/10.1016/j.nima.2017.02.009>
11. F. Yan, H.P. Geng, C. Meng et al., Commissioning experiences with the spoke-based CW superconducting proton linac. *Nucl. Sci. Tech.* **32**, 105 (2021). <https://doi.org/10.1007/s41365-021-00950-7>
12. M. Martinello, D. Bice, C. Boffo et al., Q-factor optimization for high-beta 650 MHz cavities for PIP-II. *J. Appl. Phys.* **130**, 174501 (2021). <https://doi.org/10.1063/5.0068531>
13. K. Saito, H. Inoue, E. Kako et al., Superiority of electropolishing over chemical polishing on high gradients. in *Proceedings of the 1997 Workshop on RF Superconductivity, Abano Terme, Padova, Italy* (1997), pp. 795–813
14. L. Lilje, D. Reschke, K. Twarowski et al., Electropolishing and in-situ baking of 1.3 GHz niobium cavities, in *Proceedings of the 1999 Workshop on RF Superconductivity, La Fonda Hotel, Santa Fe, New Mexico, USA* (1999), pp. 74–76
15. A. Grassellino, A. Romanenko, D. Sergatskov et al., Nitrogen and argon doping of niobium for superconducting radio frequency cavities: a pathway to highly efficient accelerating structures. *Supercond. Sci. Technol.* **26**, 102001 (2013). <https://doi.org/10.1088/0953-2048/26/10/102001>
16. S. Posen, A. Romanenko, A. Grassellino et al., Ultralow surface resistance via vacuum heat treatment of superconducting radio-frequency cavities. *Phys. Rev. Applied* **13**, 014024 (2020). <https://doi.org/10.1103/PhysRevApplied.13.014024>
17. H. Ito, H. Araki, K. Takahashi et al., Influence of furnace baking on Q-E behavior of superconducting accelerating cavities. *Prog. Theor. Exp. Phys.* **2021**, 071G01 (2021). <https://doi.org/10.1093/ptep/ptab056>
18. R.L. Geng, G.V. Ereemeev, H. Padamsee et al., High gradient studies for ILC with single-cell re-entrant shape and elliptical shape cavities made of fine-grain and large-grain niobium, in *Proceedings of PAC07, Albuquerque, New Mexico, USA* (2007), pp. 2337–2339
19. T. Kubo, Y. Ajima, H. Inoue et al., In-house production of a large-grain single-cell cavity at cavity fabrication facility and results of performance tests, in *Proceedings of IPAC2014, Dresden, Germany* (2014), pp. 2519–2521
20. S. Posen, A. Cravatta, M. Checchin et al., High gradient performance and quench behavior of a verification cryomodule for a high energy continuous wave linear accelerator. *Phys. Rev. Accel. Beams* **25**, 042001 (2022). <https://doi.org/10.1103/PhysRevAccelBeams.25.042001>
21. F.S. He, W.M. Pan, P. Sha et al., Medium-temperature furnace baking of 1.3 GHz 9-cell superconducting cavities at IHEP. *Supercond. Sci. Technol.* **34**, 095005 (2021). <https://doi.org/10.1088/1361-6668/ac1657>
22. The CEPC Study Group, CEPC conceptual design report: volume I—accelerator (2018). [arXiv:1809.00285](https://arxiv.org/abs/1809.00285)
23. J. Zhai, D. Gong, H. Zheng et al., Design of CEPC superconducting RF system. *Int. J. Mod. Phys. A* **34**, 1940006 (2019). <https://doi.org/10.1142/S0217751X19400062>
24. S. Jin, P. Sha, W. Pan et al., Development and vertical tests of CEPC 650 MHz single-cell cavities with high gradient. *Materials* **14**, 7654 (2021). <https://doi.org/10.3390/ma14247654>
25. T. Huang, W. Pan, G. Wang et al., The development of the 499.8 MHz superconducting cavity system for BEPCII. *Nucl. Instrum. Methods Phys. Res. A* **1013**, 165649 (2021). <https://doi.org/10.1016/j.nima.2021.165649>
26. Y. Huang, L. Liu, T. Jiang et al., 650 MHz elliptical superconducting RF cavities for CiADS project. *Nucl. Instrum. Methods Phys. Res. A* **988**, 164906 (2021). <https://doi.org/10.1016/j.nima.2020.164906>
27. F. Schlander, C. Darve, N. Elias et al., The superconducting accelerator for the ESS project, in *Proceedings of the SRF2017, Lanzhou, China* (2017), pp. 24–28
28. J. Knobloch, R.L. Geng, M. Liepe et al., High-field Q slope in superconducting cavities due to magnetic field enhancement at grain boundaries, in *Proceedings of the 1999 Workshop on RF Superconductivity, La Fonda Hotel, Santa Fe, New Mexico, USA* (1999), pp. 77–91
29. T. Kubo, Magnetic field enhancement at a pit on the surface of a superconducting accelerating cavity. *Prog. Theor. Exp. Phys.* **2015**, 07G301 (2015). <https://doi.org/10.1093/ptep/ptv088>
30. C. Xu, C.E. Reece, M.J. Kelley, Simulation of nonlinear superconducting rf losses derived from characteristic topography of etched and electropolished niobium surfaces. *Phys. Rev. Accel. Beams* **19**, 033501 (2016). <https://doi.org/10.1103/PhysRevAccelBeams.19.033501>
31. A. Romanenko, A. Grassellino, A.C. Crawford et al., Ultra-high quality factors in superconducting niobium cavities in ambient magnetic fields up to 190 mG. *Appl. Phys. Lett.* **105**, 234103 (2014). <https://doi.org/10.1063/1.4903808>
32. S. Huang, T. Kubo, R.L. Geng, Dependence of trapped-flux-induced surface resistance of a large-grain Nb superconducting radio-frequency cavity on spatial temperature gradient during cooldown through T_c. *Phys. Rev. Accel. Beams* **19**, 082001 (2016). <https://doi.org/10.1103/PhysRevAccelBeams.19.082001>
33. H. Padamsee, *RF superconductivity: science, technology and applications* (WILEY-VCH Verlag GmbH & Co. KGaA, Weinheim, 2009). (ISBN 978-3-527-40572-5)
34. T. Kubo, A. Gurevich, Field-dependent nonlinear surface resistance and its optimization by surface nanostructuring in superconductors. *Phys. Rev. B* **100**, 064522 (2019). <https://doi.org/10.1103/PhysRevB.100.064522>
35. A. Gurevich, T. Kubo, J.A. Sauls, Challenges and opportunities of SRF theory for next generation particle accelerators. [arXiv:2203.08315](https://arxiv.org/abs/2203.08315)
36. M. Martinello, M. Checchin, A. Romanenko et al., Field-enhanced superconductivity in high-frequency niobium accelerating cavities. *Phys. Rev. Lett.* **121**, 224801 (2018). <https://doi.org/10.1103/PhysRevLett.121.224801>
37. F. Furuta, D.J. Bice, A.C. Crawford et al., Fermilab EP facility improvement, in *Proceedings of SRF'19, Dresden, Germany* (2019). <https://accelconf.web.cern.ch/srf2019/papers/tup022.pdf>
38. M. Checchin, *LCLS-II investigation of failed LCLS-II HE prototype cavities EP analysis, TTC 2020* (Switzerland, Geneva, 2020)

Springer Nature or its licensor holds exclusive rights to this article under a publishing agreement with the author(s) or other rightsholder(s); author self-archiving of the accepted manuscript version of this article is solely governed by the terms of such publishing agreement and applicable law.